ACS SENSORS

pubs.acs.org/acssensors Article

D-Amino Acid-Based Antifouling Peptides for the Construction of Electrochemical Biosensors Capable of Assaying Proteins in Serum with Enhanced Stability

Shuju Zhao, Xiujuan Qiao, Min Chen, Yanxin Li, Xin Wang, Zhenying Xu, Yumin Wu,* and Xiliang Luo*

Cite This: *ACS Sens.* 2022, 7, 1740−1746 Read Online

ACCESS | Metrics & More | Article Recommendations | Supporting Information

ABSTRACT: The susceptibility of peptides to proteolytic degradation in human serum significantly hindered the potential application of peptide-based antifouling biosensors for long-term assaying of clinical samples. Herein, a robust antifouling biosensor with enhanced stability was constructed based on peptides composed of D-amino acids (D-peptide) with prominent proteolytic resistance. The electrode was electropolymerized with poly(3,4-ehtylenedioxythiophene) and electrodeposited with Au nanoparticles (AuNPs), and the D-peptide was then immobilized onto the AuNPs, and a typical antibody specific for immunoglobulin M (IgM) was immobilized. Because of the effect of D-amino acids, the D-peptide-modified electrode surface showed prominent antifouling capability and high tolerance to enzymatic hydrolysis. Moreover, the D-peptide-modified electrode exhibited much stronger long-term stability, as well as antifouling ability in human serum than the electrode modified with normal peptides. The electrochemical biosensor exhibited a sensitive response to IgM linearly within the range of 100 pg mL^{-1} to 1.0 μg mL^{-1} and a very low detection limit down to 37 pg mL^{-1}, and it was able to detect IgM in human serum with good accuracy. This work provided a new strategy to develop robust peptide-based biosensors to resist the proteolytic degradation for practical application in complex clinical samples.

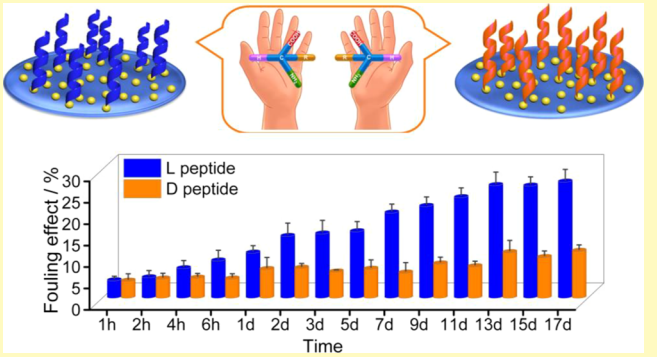

KEYWORDS: *D-amino acid, antifouling electrochemical biosensor, proteolytic degradation, immunoglobulin M (IgM), human serum*

Electrochemical sensors offer a potential application for early diagnostics and medical monitoring owing to their high sensitivity, easy processing, and low cost.[1,2] The successful practical application requires them to be long-term sustainable to resist nonspecific adsorption availably in a complex biological environment (such as serum, urine, saliva, etc.).[3−5] However, satisfying the abilities of both antifouling and long-time monitoring in situ via electrode surface controllable modification remains one of the challenges.[6]

To this end, various physical and chemical strategies were designed to prevent foulants from attachments based on such mechanisms including the hydration layer, steric repulsion, electrostatic repulsion, and surface topography.[7] Although the physical strategies based on a super-hydrophobic surface are quite stable in aqueous environments by the entropy reduction, such entropy-driven hydrophobic interactions are irreversible. To solve this problem, the hydrophilic materials were used by providing biocompatible antifouling coatings, such as polyethylene glycol-based molecules,[8,9] sulfobetaine,[10] phosphorylcholine,[11] and zwitterionic peptides.[12−14] Among them, peptide-based materials have gained much attention because of their tunable structural characteristic, biocompatibility, low toxicity, and ease of synthesis.[15] The zwitterionic peptide flanked alternatively with positively and negatively charged amino acid such as ER,[16] EK,[17] and NQ[18] offers superior surface hydration, weak binding with other proteins, and outstanding antifouling behavior (E: glutamic; K: lysine; R: arginine; N: aspargine; Q: glutamine). For example, the zwitterionic peptide composed of E and K has been reported to resist nonspecific interactions by Nowinski et al.[19] and Chen et al.[20]

Despite peptides' favorable antifouling property, the activity of proteolytic enzymes limits peptide antifouling-based electrochemical sensor performance in complicated environments.[21−24] Therefore, the regulation measures extremely need to improve their tolerance of antifouling coating with

Received: March 11, 2022
Accepted: May 18, 2022
Published: May 26, 2022

continuous long-term monitoring in vitro. Until now, significant strategies to protect biologically active peptides from enzymatic decomposition have been adopted to enhance the biological stability of various peptides, such as the conjugation of cyclization[25] and the incorporation of unnaturally prepared amino acids,[26,27] such as D-amino acid,[28] 2-aminoisobutric acid,[29] and β-amino acid.[30] Among them, D-amino acid is an alternative approach to confer proteolytic resistance.[31] Its stability toward enzymatic degradation with desired activity has progressively gained much attention.[32,33] For example, Tugyi and co-workers[26] reported that the substitutions of D-amino acid at the ends of the L-peptide (tpTPTGTQtpt) improved the stability of the peptide to proteolysis and prolonged the biological half-time in human serum. Lu et al.[33] also reported that the application of D-amino acid in antimicrobial peptides displayed remarkable stability against proteolytic degradation and mild toxicity. Hong et al.[34] indicated that all D-amino acid substitutions enhanced the activity of antimicrobial peptides in vivo despite the changed secondary structure of peptides.

Inspired by the above information, it is possible to achieve continuous long-term monitoring in situ by controllable construction of a peptide-based electrochemical biosensor with an excellent antifouling property and favorable resistance to enzymatic decomposition. In this work, the controllable strategies of adopting D-amino acid as the hydrophilic core have been applied to design a linear antifouling peptide (cppppekekekek) to support the low fouling and robust biosensing of proteins in human serum. The D-amino acid-based peptide (D-peptide) was further immobilized on the AuNPs/PEDOT-modified electrode surface, and the IgM antibody was subsequently immobilized onto the antifouling peptide layer to construct the biosensor.[17,35] Owing to the existence of the D-peptide with a good antifouling property, the developed electrochemical biosensors exhibited long-term stability and high antifouling performance in human serum.

EXPERIMENTAL SECTION

Materials and Reagents. Synthesis of the designed peptide cppppekekekek and the peptide CPPPPEKEKEKEK (the small letters and capital letters stand for the D-amino acids and L-amino acids, respectively) was accomplished by Bankpeptide Biological Technology Co. Ltd. (Hefei, China). Human immunoglobulin M (IgM) and IgM antibody (Ab) were purchased from Sangon Biotech Co., Ltd. (Shanghai, China). Poly(sodium 4-styrenesulfonate) (PSS) and 3,4-ethyl-enedloxythlophene ($C_6H_6O_2S$, EDOT) were bought from Aladdin Biochemical (Shanghai, China). *N*-Hydroxysuccinimide (NHS) and 1-ethyl-3-(3-dimethylaminopropyl) carbodiimide (EDC) were obtained from Sigma-Aldrich (St. Louis, MO, USA). The pure protein bovine serum albumin (BSA), myoglobin (Mb), and lysozyme (Lys) were provided by Beijing Xinke Zhongjing Bijotechnology Co., Ltd. (Beijing, China). Fluorescein isothiocyanate FITC-BSA was offered by Bo Yang Hongda Technology (Beijing, China). Other analytical chemicals were ordered from the BBI Life Sciences Corporation (Shanghai, China). Human sera of patients and healthy persons were donated by the Eighth People's Hospital of Qingdao (Qingdao, China). All clinical samples were authorized by the hospital's institutional review board and used according to the laws and guidelines. Ultrapure water was produced by the Milli-Q water purification equipment (resistivity > 18 MΩ·cm^{-1}).

Apparatus. All electrochemical tests were conducted using CHI 660E electrochemical workstations (Shanghai CH Instrument Co., China) at room temperature. A classical three-electrode system included a glassy carbon electrode (GCE, diameter of 3.0 mm) used as the working electrode, and the saturated calomel electrode (CHI 150) and the platinum wire worked as the reference and the auxiliary electrodes, respectively. Cyclic voltammetry (CV) was performed with a scan rate of 100 mV·S^{-1}, and differential pulse voltammetry (DPV) measurements were performed in the range of −0.2 to 0.6 V, with 50 mV amplitude. All electrochemical experiments were performed in the 10 mM phosphate buffered saline (PBS, pH 7.4) containing 0.1 M KCl and 5.0 mM $[Fe(CN)_6]^{3-/4-}$. X-ray photoelectron spectrometry (XPS) was performed using an ESCALAB 250Xi spectrometer (Thermo VG Fisher Scientific, USA). Scanning electron microscopy (SEM) for the characterization of the modified electrode surface was performed using the SEM instrument JEOL JSM-7500F (Hitachi High-Technology Co., Ltd., Japan). Circular dichroism (CD) data of the peptides were measured using a JASCO J-810 spectropolarimeter (JASCO Inc., Japan). The hydrophilicity of the modified surface was recorded with a JC2000D1 Instrument (Zhongchen Instrument Co., Shanghai, China). The confocal images of protein adsorption were collected using a TCS-SP5 confocal laser microscope (Leica, Germany). The evaluation of zeta potential (ζ) was measured using the Zetasizer Nano-ZS Instrument (Malvern Instruments, USA).

Characterization of D-Peptides. CD spectroscopy to reveal the peptide's secondary structure was performed within the range of 190−300 nm, with 0.5 nm step resolution in peptide solutions (0.3 mg·mL^{-1}). Peptide charges were evaluated by zeta potential measurements and the utilization of calculation method. The hydrophilic property of peptide-grafted surfaces was characterized by measuring the water contact angle.

Fabrication of the AuNPs/PEDOT/GCE Modified Surface. The bare GCE was polished using Al_2O_3 powders (0.3 and 0.05 μm, respectively) and washed with ultrasonication using water, ethanol, and again water for 2−3 min, respectively. The PEDOT film was electrodeposited on the GCE by the *i*−*t* amperometric electrodeposition technique (with a potential of 1.0 V, 20 s) in the solution containing EDOT (0.02 M) and PSS (2.0 mg·mL^{-1}) according to previous reports.[36,37] The subsequent electrochemical formation of AuNPs was performed using the CV method (−1.5 to 0.5 V, with a scan rate of 50 mV·S^{-1}, six segments) in 0.5 mM $HAuCl_4$ solution with 0.5 M KNO_3.[38]

Preparation of the Electrochemical Biosensor. The biosensor construction procedure is shown in Scheme 1. The AuNPs/PEDOT/GCE was incubated in D-peptide solution (0.2 mg·mL^{-1}) for 12 h to immobilize peptides onto the electrode surface. The electrode was immersed in the fresh solution of 0.1 M NHS and 0.4 M EDC (adjust pH to 5.5−6.0 with 0.1 M HCl) for 0.5 h. After washing with water, the electrode was further incubated for 2 h within IgM antibody solution (1.0 μg mL^{-1}, in 10 mM PBS with pH 7.4). The prepared biosensor was stored in the PBS prior to measurement.

Scheme 1. Schematic Construction Process of the Antifouling Biosensor

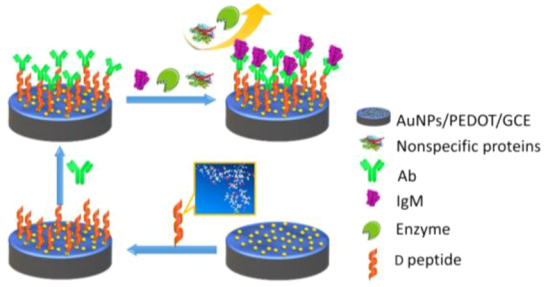

Antifouling Performance Evaluation. The antifouling properties of different electrodes were first assessed using different single protein solutions, such as negative BSA, positive Lys, and neutral Mb, respectively. In addition, the antifouling evaluation was also carried out in complex media of human serum. The DPV signal change rates of various electrodes were recorded to assess the antifouling performance after electrode immersion in different protein and

https://doi.org/10.1021/acssensors.2c00518
ACS Sens. 2022, 7, 1740−1746

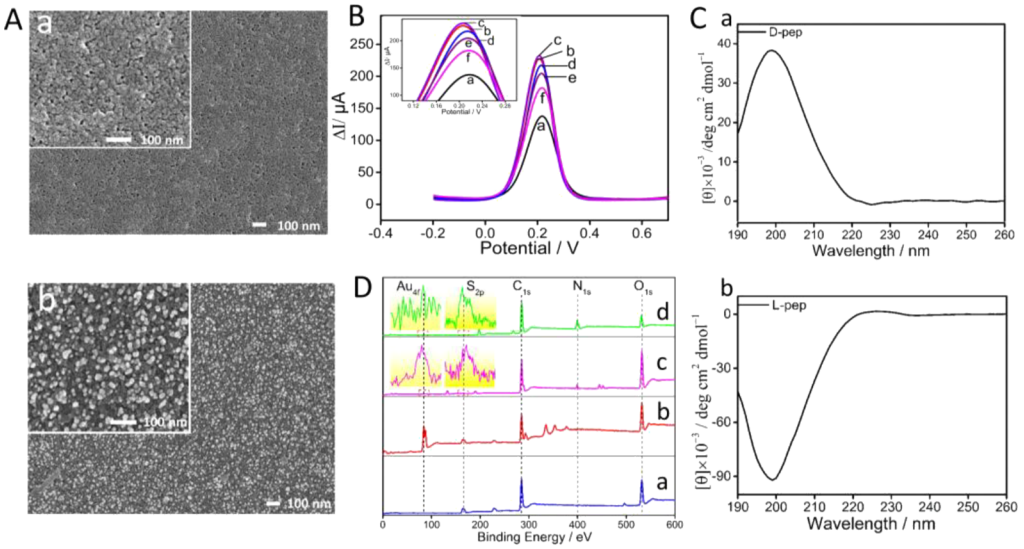

Figure 1. (A)SEM images of the PEDOT (a) and AuNPs/PEDOT (b) modified electrode surfaces. Insets show the corresponding zoomed images. (B) DPV curves of (a) bare GCE and GCEs modified with (b) PEDOT, (c) AuNPs/PEDOT, (d) D-pep/AuNPs/PEDOT, (e) Ab/D-pep/AuNPs/PEDOT, and (f) IgM/Ab/D-pep/AuNPs/PEDOT in PBS with 5.0 mM redox probe $[Fe(CN)_6]^{3-/4-}$. Inset shows the zoomed part of the Figure. (C) CD spectra of (a) D-peptide and (b) L-peptide. (D) XPS characterization of GCE surfaces modified with (a) PEDOT, (b) AuNPs/PEDOT, (c) D-pep/AuNPs/PEDOT, and (d) Ab/D-pep/AuNPs/PEDOT.

serum samples for 0.5 h. Similarly, the long-term antifouling performance was tested in 20% human serum.

Detection of IgM. The electrochemical biosensor was immersed in IgM solutions or clinical samples for 60 min at ambient temperature, and after the binding of IgM to the IgM antibody, the biosensor was rinsed and then immersed in PBS with 5.0 mM $[Fe(CN)]^{3-/4-}$ to record the DPV response. The DPV responses of the biosensor before and after target incubation were respectively recorded. To further assess the utilization potentiality and reliability of the fabricated biosensor, clinical human sera were analyzed by the prepared biosensors (considering the biosensor detection range, the clinical human sera were carefully diluted using 10 mM PBS if necessary), and the obtained data were then compared with those tested with the enzyme-linked immunosorbent assay (ELISA) kits.

RESULTS AND DISCUSSION

PROPERTY INVESTIGATION OF THE DESIGNED D-PEPTIDE

The chromatography and mass spectra of the D- and L-peptides are demonstrated in Figures S1 and S2, which verified the successful synthesis of the peptides. Hydrogen bonding prevents the surface of the peptide from protein adsorption and further resists biofouling by the formation of a steric barrier. Ionic solvation and charge balance strengthen the hydration of zwitterionic peptides.[15] Herein, the peptide hydration ability was revealed by water contact angle and peptide charge calculation. As illustrated in Figure S3, the contact angles of the GCE, the AuNPs/PEDOT, L-pep/AuNPs/PEDOT, and D-pep/AuNPs/PEDOT-modified electrodes were 65.2°, 45.6°, 24.8°, and 21.4°, respectively. These results indicated that the D-peptide had similar strong water binding ability compared with the L-peptide. The calculation result is displayed in Figure S4A, and the net charge of the designed peptide was near to zero at pH 7.0. The zeta potential was measured in the peptide solution (Figure S4B). The zeta potential was about 7.8 mV for the D-peptide, indicating a slightly positive charge. The above results indicated that the D-peptide possessed good hydrophilicity and was nearly neutral, which is favorable for antifouling applications.

The CD results of the secondary structures of the D-peptide and L-peptide (0.5 mg·mL^{-1}) in water are shown in Figure 1C. In stark contrast to the L-peptide, the CD spectrum of the D-peptide exhibited a strong positive band at about 200 nm and a negative band at 225 nm.[19] This result indicated the formation of a successive four-polyproline helix structure.[39] The conformation of this rigid structure has a profound effect on the antifouling property of well-packed peptide layers.[19]

Investigation of the Biosensor Construction Process. With regard to the construction of the electrochemical biosensor, the GCE was electrodeposited with PEDOT and AuNPs in sequence. The AuNPs/PEDOT film worked as a conductive substrate, and it also assisted the immobilization of the peptide. SEM images of the modified electrode surfaces were recorded (Figure 1A). Clearly, the PEDOT electrodeposited on the electrode possessed a rough surface, and the AuNPs with diameters of 20∼50 nm were decorated on the PEDOT film.

The DPV response curves of various electrodes were measured in PBS with the redox probe $[Fe(CN)_6]^{3-/4-}$, as depicted in Figure 1B. The DPV current of the electrode increased consecutively after the deposition of conductive PEDOT and AuNPs, owing to their favorable electrical conductivity and big surface area, while the peak current decreased remarkably with the immobilization of the peptide and the IgM antibody, as the nonconductive biomolecules hindered the electron transfer. The peak current further decreased with the specific binding of the IgM, and this current change provided a useful signal for the target detection.

XPS was employed to check the element change during the biosensor fabrication process (Figure 1D). The carbon (C), sulfur (S), and oxygen (O) as typical elements for PEDOT appeared at 163.88 eV (S_{2p}), 284.68 eV (C_{1s}), and 532.98 eV (O_{1s}), respectively (curve a), demonstrating the successful electrodeposition of PEDOT.[40] A new peak at 84.03 eV corresponding to the gold nanoparticles (Au_{4f}) was observed

https://doi.org/10.1021/acssensors.2c00518
ACS Sens. 2022, 7, 1740−1746

for the AuNPs/PEDOT/GCE (curve b). After the self-assembly of peptides, a characteristic element of nitrogen (N_{1s}) appeared at 399.71 eV[41] (curve c). Furthermore, the peak of nitrogen increased distinctly associated with the immobilization of the IgM antibody (curve d), owing to the abundant nitrogen element of the antibody. The XPS characterization also confirmed the successful construction of the biosensor.

Antifouling Performance Assessment. The antifouling performances of different electrodes were evaluated through the measurement of DPV responses before (I_0) and after (I) soaking in biological samples (Pure proteins: Mb with neutral charge, Lys with positive charge and BSA with negative charge) for half an hour. As displayed in Figure S5, the DPV peaks of the bare GCEs sharply decreased after soaking in protein solutions, mainly due to the adsorption of nonconductive proteins that blocked the surface of the electrode. The D-peptide (Figure S5A″, B″, C″) and L-peptide (Figure S5 A‴, B‴, C‴) modified electrodes displayed outstanding antifouling performances with less protein adsorption, owing to their conterminal hydration of E and K amino acids with the generation of hydrogen bonds and hydrophilic forces through combining water molecules.[42] Given the mirror image of side-chain orientations in the enantiomeric peptides, the D-peptide also exhibited a similar closely packed hydration layer, and the D-peptide and L-peptide exhibited similar antifouling performances.

The peptide stability has a profound effect on its antifouling property in a complex environment, especially in clinical human serum because of the presence of endopeptidase and exopeptidase, such as trypsin, chymotrypsin, aminopeptidase, and carboxypeptidase. Compared with the L-peptide, the D-peptide has enhanced stability because of its proteolytic resistance.[43] Herein, the contrastive antifouling assessment of D-peptide- and L-peptide-modified electrodes was performed in human serum, as shown in Figure 2A. Clearly, the D-peptide- and L-peptide-modified electrodes showed no significant differences in antifouling performance after incubation in various human serum samples for 30 min. The signal suppression of electrodes modified with D- and L-peptides was only 5.7 and 6.2% after soaking in 20% sera, respectively. Though it is reported that the introduction of D-amino acid might lead to some changes in the peptide's physicochemical properties, like conformation, solubility, and stability,[44] there is no significant effect on the hydration of the amino and carboxyl groups and the antifouling performance.

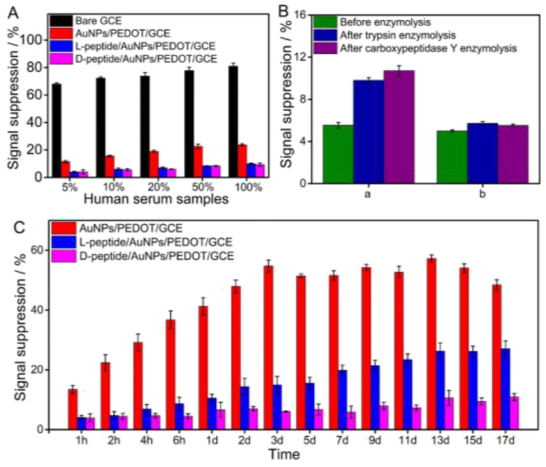

Figure 2. (A) Comparison of the antifouling abilities of various electrodes after incubation in different human serum samples for 30 min. (B) Antifouling abilities of AuNPs/PEDOT/GCE modified with L-peptide (a) and D-peptide (b) tested in 20% serum samples, with or without enzyme hydrolysis in 0.02 mg mL^{-1} trypsin or carboxypeptidase Y. (C) Long-term antifouling measurements of various electrodes tested in 20% serum samples.

To confirm the advantage of the D-peptide to resist enzymatic degradation, the tolerance of the peptide to enzymolysis was investigated by assessing the antifouling abilities of the peptide-modified electrodes after soaking in endopeptidase and exopeptidase solutions. The electrodes modified with the D-peptide and L-peptide were soaked in trypsin solution (0.02 mg mL^{-1}) for 4 h at 37 °C and then dipped in 20% serum samples for 30 min. As depicted in Figure 2B, after the enzymolysis treatment, the D-peptide-modified electrode exhibited a small change in signal suppression, but that of the electrode modified with the L-peptide clearly increased to 9.8%, owing to the degradation of the L-peptide and the weakened antifouling performance. The result certified that the D-peptide exhibited predominant hindrance to endopeptidase hydrolysis. The carboxypeptidase Y was further used to investigate the carboxypeptidase tolerance of the peptides (Figure 2B). Similarly, the D-peptide-modified electrode showed a slight change after enzymolysis for 4 h, while the L-peptide-modified electrode exhibited a sharp increase of the signal suppression to 11.2%. These results demonstrated that the designed D-peptide had prominent stability in human serum on account of the excellent resistance to endopeptidase and exopeptidase, which is similar to previous reports.[45]

The antifouling performance of the peptide-modified surfaces was further investigated with confocal images using FITC-BSA (Figure S6). The images of the D-peptide-modified surfaces showed no significant changes of BSA adsorption after trypsin and carboxypeptidase Y treatments. However, owing to enzymatic degradation, the L-peptide-modified surfaces showed obvious enhancement in BSA adsorption (reduced antifouling performance) after trypsin and carboxypeptidase Y treatment. Both the electrochemical and fluorescence tests reflected that the D-peptide exhibited enhanced stability and tolerance to enzymolysis in biological media.

The long-term antifouling abilities of various electrodes in a complex environment were also investigated (Figure 2C). The electrode modified with the L-peptide showed a signal suppression increase up to 14.4%, while the D-peptide-modified electrode kept at 6.9% in 2 days. It is worth mentioning that there was a continuously increasing trend for the L-peptide-modified electrode up to 27.1%, while the signal suppression of the D-peptide-modified electrode remained steadily less than 12.0% after 17 days, indicating a favorable long-term antifouling performance.

Detection of IgM. IgM is of significance in primary viral infections and bloodstream infections, and the IgM detection is based on the interaction between IgM and its antibody with a reaction time of 1 h.[46] Under the optimized conditions (Figure S7), the electrochemical biosensor response to IgM in 10 mM PBS was illustrated in Figure 3A, B. Within the linear range between 100 pg·mL^{-1} and 1.0 μg·mL^{-1}, the linear equation was obtained as ΔI (μA) = 5.03LgC_{IgM} + 57.18 (R^2 = 0.9998), and the detection limit was 33.7 pg·mL^{-1} (with the S/N of 3).

https://doi.org/10.1021/acssensors.2c00518
ACS Sens. 2022, 7, 1740−1746

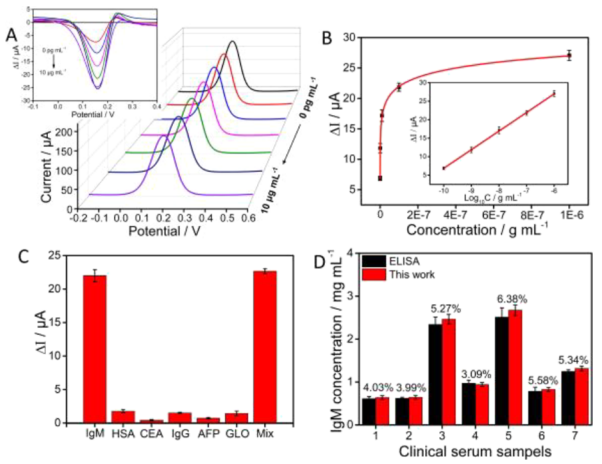

Figure 3. (A) DPV curves of the electrochemical biosensor to various concentrations of IgM (0, 0.1, 1.0, 10, 100, 1000, and 10,000 ng·mL^{-1}). Insert: DPV responses with the background subtracted. (B) Corresponding biosensor responses to different concentrations of IgM. Inset: the corresponding linear calibration curve. (C) Biosensor responses to 100 ng·mL^{-1} IgM, 10 μg mL^{-1} of HSA, CEA, IgG, AFP, and GLO, and the mixture, respectively. (D) Clinical serum sample analysis results obtained with the biosensor and the ELISA method. The differences between the measuring results of these two methods are indicated.

Selectivity, Stability, and Reproducibility Investigation. To evaluate the selectivity, the biosensor was used to measure 100 ng·mL^{-1} target IgM, and 10 μg·mL^{-1} interferons of HSA, CEA, IgG, AFP, GLO, and their mixed solution (Figure 3C). The biosensor DPV responses to these nonspecific proteins were considerably lower than its response to IgM, although the concentrations of those proteins were 100 times higher than that of IgM. It is clear that this biosensor possessed excellent selectivity.

CV scanning and DPV measurement were adopted to investigate the biosensor stability (Figure S8). The CV peak current of the biosensor varied slightly with 100 repeated sweep segments (Figure S8A), and the DPV responses remained almost unchanged within 15 days (Figure S8B). For the reproducibility test, seven independently prepared biosensors were used to measure IgM solutions with the same concentration, and no significant changes in biosensor responses were observed, with the relative standard deviation under 7.3% (Figure S8C). These results illustrated the prominent stability and reproducibility of the biosensor.

Analysis of Clinical Samples. The pragmatic application of the antifouling biosensor was inspected with clinical serum samples. In view of the high IgM concentration in human serum (0.39−2.83 mg mL^{-1}), and the linear detection range of the prepared antifouling biosensor, the clinical samples need to be diluted before assay. As displayed in Figure 3D, the concentration of IgM in clinical samples was detected by the biosensor and ELISA method, respectively. The percentage of variances between the measured results of these two methods for all the clinical samples was within 6.5%. These results revealed that the fabricated antifouling biosensor based on the D-peptide was suitable for practical detection of real samples with acceptable accuracy.

CONCLUSIONS

In conclusion, an antifouling biosensor with enhanced stability in complex human serum was prepared based on the designed D-peptide. The D-peptide displayed prominent stability in human serum owing to its strong enzymatic degradation resistance to active endopeptidase and exopeptidase. In the meantime, the D-peptide exhibited similar antifouling capability to its corresponding L-peptide. However, the D-peptide-based electrochemical biosensor possessed high stability, sensitivity, and selectivity, and it was capable of measuring IgM target in practical serum samples, without biofouling and with satisfactory accuracy. This strategy of designing D-peptides for the preparation of antifouling biosensors can be adopted to develop various biosensors with robust performances in complex biological samples.

ASSOCIATED CONTENT

Supporting Information

The Supporting Information is available free of charge at https://pubs.acs.org/doi/10.1021/acssensors.2c00518.

Chromatogram and MS spectrum of the D-peptide and L-peptide, contact angle of photographs, zeta potential, structure of the D-peptide, antifouling ability in pure proteins, stability of the modified electrodes, confocal imaging of FITC-BSA protein adsorption, and reproducibility of the biosensor (PDF)

AUTHOR INFORMATION

Corresponding Authors

Yumin Wu − *State Key Laboratory Base of Eco-chemical Engineering, Key Laboratory of Optic-Electric Sensing and Analytical Chemistry for Life Science, MOE, College of Chemistry and Molecular Engineering, Qingdao University of Science & Technology, Qingdao 266042, China;* orcid.org/0000-0002-6941-6130; Email: wuyumin005@163.com

Xiliang Luo − *State Key Laboratory Base of Eco-chemical Engineering, Key Laboratory of Optic-Electric Sensing and Analytical Chemistry for Life Science, MOE, College of Chemistry and Molecular Engineering, Qingdao University of Science & Technology, Qingdao 266042, China;* orcid.org/0000-0001-6075-7089; Email: xiliangluo@qust.edu.cn

Authors

Shuju Zhao − *State Key Laboratory Base of Eco-chemical Engineering, Key Laboratory of Optic-Electric Sensing and Analytical Chemistry for Life Science, MOE, College of Chemistry and Molecular Engineering, Qingdao University of Science & Technology, Qingdao 266042, China*

Xiujuan Qiao − *State Key Laboratory Base of Eco-chemical Engineering, Key Laboratory of Optic-Electric Sensing and Analytical Chemistry for Life Science, MOE, College of Chemistry and Molecular Engineering, Qingdao University of Science & Technology, Qingdao 266042, China*

Min Chen − *State Key Laboratory Base of Eco-chemical Engineering, Key Laboratory of Optic-Electric Sensing and Analytical Chemistry for Life Science, MOE, College of Chemistry and Molecular Engineering, Qingdao University of Science & Technology, Qingdao 266042, China*

Yanxin Li − *State Key Laboratory Base of Eco-chemical Engineering, Key Laboratory of Optic-Electric Sensing and*

https://doi.org/10.1021/acssensors.2c00518
ACS Sens. 2022, 7, 1740−1746

Analytical Chemistry for Life Science, MOE, College of Chemistry and Molecular Engineering, Qingdao University of Science & Technology, Qingdao 266042, China

Xin Wang − *State Key Laboratory Base of Eco-chemical Engineering, Key Laboratory of Optic-Electric Sensing and Analytical Chemistry for Life Science, MOE, College of Chemistry and Molecular Engineering, Qingdao University of Science & Technology, Qingdao 266042, China*

Zhenying Xu − *State Key Laboratory Base of Eco-chemical Engineering, Key Laboratory of Optic-Electric Sensing and Analytical Chemistry for Life Science, MOE, College of Chemistry and Molecular Engineering, Qingdao University of Science & Technology, Qingdao 266042, China*

Complete contact information is available at: https://pubs.acs.org/10.1021/acssensors.2c00518

Author Contributions

The manuscript was written through contributions of all authors. All authors have given approval to the final version of the manuscript.

Notes

The authors declare no competing financial interest.

■ ACKNOWLEDGMENTS

We acknowledge the financial support from the National Natural Science Foundation of China (21974075 and 22174082), the Taishan Scholar Program of Shandong Province of China (ts20110829), and the Science and Technology Benefiting the People Project of Qingdao (20-3-4-53-nsh).

■ REFERENCES

(1) Lin, P.-H.; Li, B.-R. Antifouling strategies in advanced electrochemical sensors and biosensors. *Analyst* **2020**, *145*, 1110−1120.

(2) Castle, L. M.; Schuh, D. A.; Reynolds, E. E.; Furst, A. L. Electrochemical sensors to detect bacterial foodborne pathogens. *ACS Sens.* **2021**, *6*, 1717−1730.

(3) Jiang, C.; Wang, G.; Hein, R.; Liu, N.; Luo, X.; Davis, J. J. Antifouling Strategies for Selective In Vitro and In Vivo Sensing. *Chem. Rev.* **2020**, *120*, 3852−3889.

(4) Wang, W.; Han, R.; Chen, M.; Luo, X. Antifouling peptide hydrogel based electrochemical biosensors for highly sensitive detection of cancer biomarker HER2 in human serum. *Anal. Chem.* **2021**, *93*, 7355−7361.

(5) Campuzano, S.; Pedrero, M.; Yáñez-Sedeño, P.; Pingarrón, J. M. Antifouling (bio) materials for electrochemical (bio)sensing. *Int. J. Mol. Sci.* **2019**, *20*, 423.

(6) Cui, M.; Ma, Y.; Wang, L.; Wang, Y.; Wang, S.; Luo, X. Antifouling sensors based on peptides for biomarker detection. *TrAC-Trend. Anal. Chem.* **2020**, *127*, No. 115903.

(7) Russo, M. J.; Han, M.; Desroches, P. E.; Manasa, C. S.; Dennaoui, J.; Quigley, A. F.; Kapsa, R. M. I.; Moulton, S. E.; Guijt, R. M.; Greene, G. W.; Silva, S. M. Antifouling strategies for electrochemical biosensing: mechanisms and performance toward point of care based diagnostic applications. *ACS Sens.* **2021**, *6*, 1482−1507.

(8) Jolly, P.; Miodek, A.; Yang, D.-K.; Chen, L.-C.; Lloyd, M. D.; Estrela, P. Electro-engineered polymeric films for the development of sensitive aptasensors for prostate cancer marker detection. *ACS Sens.* **2016**, *1*, 1308−1314.

(9) Ostaci, R.-V.; Damiron, D.; Al Akhrass, S.; Grohens, Y.; Drockenmuller, E. Poly(ethylene glycol) brushes grafted to silicon substrates by click chemistry: Influence of PEG chain length, concentration in the grafting solution and reaction time. *Polym. Chem.* **2011**, *2*, 348−354.

(10) Jiang, C.; Alam, M. T.; Parker, S. G.; Darwish, N.; Gooding, J. J. Strategies to achieve control over the surface ratio of two different components on modified electrodes using aryldiazonium salts. *Langmuir* **2016**, *32*, 2509−2517.

(11) Jiang, C.; Alam, M. T.; Silva, S. M.; Taufik, S.; Fan, S.; Gooding, J. J. Unique sensing interface that allows the development of an electrochemical immunosensor for the detection of tumor necrosis factor α in whole blood. *ACS Sens.* **2016**, *1*, 1432−1438.

(12) Gu, S.; Shi, X.-M.; Zhang, D.; Fan, G.-C.; Luo, X. Peptide-Based Photocathodic Biosensors: Integrating a Recognition Peptide with an Antifouling Peptide. *Anal. Chem.* **2021**, *93*, 2706−2712.

(13) Hlídková, H.; Kotelnikov, I.; Pop-Georgievski, O.; Proks, V.; Horák, D. Antifouling Peptide Dendrimer Surface of Monodisperse Magnetic Poly(glycidyl methacrylate) Microspheres. *Macromolecules* **2017**, *50*, 1302−1311.

(14) Liu, N.; Song, J.; Lu, Y.; Davis, J. J.; Gao, F.; Luo, X. Electrochemical Aptasensor for Ultralow Fouling Cancer Cell Quantification in Complex Biological Media Based on Designed Branched Peptides. *Anal. Chem.* **2019**, *91*, 8334−8340.

(15) Sakala, G.; Reches, M. Peptide-Based Approaches to Fight Biofouling. *Adv. Mater. Interfaces* **2018**, *5*, No. 1800073.

(16) Ye, H.; Wang, L.; Huang, R.; Su, R.; Liu, B.; Qi, W.; He, Z. Superior Antifouling Performance of a Zwitterionic Peptide Compared to an Amphiphilic Non-Ionic Peptide. *ACS Appl. Mater. Interfaces* **2015**, *7*, 22448−22457.

(17) Cui, M.; Wang, Y.; Jiao, M.; Jayachandran, S.; Wu, Y.; Fan, X.; Luo, X. Mixed self-assembled aptamer and newly designed zwitterionic peptide as antifouling biosensing interface for electrochemical detection of alpha-fetoprotein. *ACS Sens.* **2017**, *2*, 490−494.

(18) Liu, N.; Hui, N.; Davis, J. J.; Luo, X. Low fouling protein detection in complex biological media supported by a designed multifunctional peptide. *ACS Sens.* **2018**, *3*, 1210−1216.

(19) Nowinski, A. K.; Sun, F.; White, A. D.; Keefe, A. J.; Jiang, S. Sequence, Structure, and Function of Peptide Self-Assembled Monolayers. *J. Am. Chem. Soc.* **2012**, *134*, 6000−6005.

(20) Chen, S.; Cao, Z.; Jiang, S. Ultra-low fouling peptide surfaces derived from natural amino acids. *Biomaterials* **2009**, *30*, 5892−5896.

(21) Kumar, P.; Takayesu, A.; Abbasi, U.; Kalathottukaren, M. T.; Abbina, S.; Kizhakkedathu, J. N.; Straus, S. K. Antimicrobial Peptide−Polymer Conjugates with High Activity: Influence of Polymer Molecular Weight and Peptide Sequence on Antimicrobial Activity, Proteolysis, and Biocompatibility. *ACS Appl. Mater. Interfaces* **2017**, *9*, 37575−37586.

(22) Kaefer, K.; Krüger, K.; Schlapp, F.; Uzun, H.; Celiksoy, S.; Flietel, B.; Heimann, A.; Schroeder, T.; Kempski, O.; Sönnichsen, C. Implantable Sensors Based on Gold Nanoparticles for Continuous Long-Term Concentration Monitoring in the Body. *Nano Lett.* **2021**, *21*, 3325−3330.

(23) Zarif, F.; Anasir, M. I.; Koh, J. X.; Chew, M.-F.; Poh, C. L. Stability and antiviral activity of SP40 peptide in human serum. *Virus Res.* **2021**, *303*, No. 198456.

(24) Schneider, S.; Ftouni, H.; Niu, S.; Schmitt, M.; Simonin, F.; Bihel, F. Rapid and scalable synthesis of innovative unnatural α,β or γ-amino acids functionalized with tertiary amines on their side-chains. *Org. Biomol. Chem.* **2015**, *13*, 7020−7026.

(25) Chan, L.; Zhang, V.; Huang, Y.-H.; Waters, N.; Bansal, P.; Craik, D.; Daly, N. Cyclization of the Antimicrobial Peptide Gomesin with Native Chemical Ligation: Influences on Stability and Bioactivity. *ChemBioChem* **2013**, 14.

(26) Tugyi, R.; Uray, K.; Iván, D.; Fellinger, E.; Perkins, A.; Hudecz, F. Partial D-amino acid substitution: Improved enzymatic stability and preserved Ab recognition of a MUC2 epitope peptide. *Proc. Natl. Acad. Sci. U. S. A.* **2005**, *102*, 413.

(27) Zhang, M.; Lu, W. Enhanced glioma-targeting and stability of LGICP peptide coupled with stabilized peptide DA7R. *Acta Pharm. Sin. B* **2018**, *8*, 106−115.

(28) Yan, L.; Ke, Y.; Kan, Y.; Lin, D.; Yang, J.; He, Y.; Wu, L. New insight into enzymatic hydrolysis of peptides with site-specific amino acid d-isomerization. *Bioorg. Chem.* **2020**, *105*, No. 104389.
(29) Beyer, C. D.; Reback, M. L.; Gopal, S. M.; Nolte, K. A.; Finlay, J. A.; Clare, A. S.; Schäfer, L. V.; Metzler-Nolte, N.; Rosenhahn, A. α-Aminoisobutyric Acid-Stabilized Peptide SAMs with Low Nonspecific Protein Adsorption and Resistance against Marine Biofouling. *ACS Sustainable Chem. Eng.* **2020**, *8*, 2665−2671.
(30) Schmitt, M. A.; Weisblum, B.; Gellman, S. H. Interplay among Folding, Sequence, and Lipophilicity in the Antibacterial and Hemolytic Activities of α/β-Peptides. *J. Am. Chem. Soc.* **2007**, *129*, 417−428.
(31) King, T. P.; Wade, D.; Coscia, M. R.; Mitchell, S.; Kochoumian, L.; Merrifield, B. Structure-immunogenicity relationship of melittin, its transposed analogues, and D-melittin. *J. Immunol.* **1994**, *153*, 1124.
(32) Zengin, A.; Cinar, G.; Guler, M. O. Controlled enzymatic stability and release characteristics of supramolecular chiral peptide amphiphile nanofiber gels. *Curr. Appl. Phys.* **2017**, *17*, 785−792.
(33) Lu, J.; Xu, H.; Xia, J.; Ma, J.; Xu, J.; Li, Y.; Feng, J. D- and Unnatural Amino Acid Substituted Antimicrobial Peptides With Improved Proteolytic Resistance and Their Proteolytic Degradation Characteristics. *Front. Microbiol.* **2020**, *11*, No. 563030.
(34) Hong, S. Y.; Oh, J. E.; Lee, K.-H. Effect of d-amino acid substitution on the stability, the secondary structure, and the activity of membrane-active peptide. *Biochem. Pharmacol.* **1999**, *58*, 1775−1780.
(35) Wang, J.; Song, J.; Yang, Z.; He, S.; Yang, Y.; Feng, X.; Dou, X.; Shan, A. Antimicrobial Peptides with High Proteolytic Resistance for Combating Gram-Negative Bacteria. *J. Med. Chem.* **2019**, *62*, 2286−2304.
(36) Chen, M.; Han, R.; Wang, W.; Li, Y.; Luo, X. Antifouling Aptasensor Based on Self-Assembled Loop-Closed Peptides with Enhanced Stability for CA125 Assay in Complex Biofluids. *Anal. Chem.* **2021**, *93*, 13555−13563.
(37) Song, Z.; Chen, M.; Ding, C.; Luo, X. Designed Three-in-One Peptides with Anchoring, Antifouling, and Recognizing Capabilities for Highly Sensitive and Low-Fouling Electrochemical Sensing in Complex Biological Media. *Anal. Chem.* **2020**, *92*, 5795−5802.
(38) Wang, G.; Han, R.; Li, Q.; Han, Y.; Luo, X. Electrochemical Biosensors Capable of Detecting Biomarkers in Human Serum with Unique Long-Term Antifouling Abilities Based on Designed Multifunctional Peptides. *Anal. Chem.* **2020**, *92*, 7186−7193.
(39) Fisher, P. J.; Prendergast, F. G.; Ehrhardt, M. R.; Urbauer, J. L.; Wand, A. J.; Sedarous, S. S.; McCormick, D. J.; Buckley, P. J. Calmodulin interacts with amphiphilic peptides composed of all D-amino acids. *Nature* **1994**, *368*, 651−653.
(40) Stockhausen, V.; Trippé-Allard, G.; Van Quynh, N.; Ghilane, J.; Lacroix, J.-C. Grafting π-Conjugated Oligomers Incorporating 3,4-Ethylenedioxythiophene (EDOT) and Thiophene Units on Surfaces by Diazonium Electroreduction. *J. Phys. Chem. C* **2015**, *119*, 19218−19227.
(41) Moulder, J. F.; Stickle, W. F.; Sobol, W. M.; Bomben, K. D. *Handbook of X-Ray Photoelectron Spectroscopy*; 1992.
(42) Zhou, L.; Li, X.; Zhu, B.; Su, B. An Overview of Antifouling Strategies for Electrochemical Analysis. *Electroanalysis* **2021**, DOI: 10.1002/elan.202100406.
(43) Zhou, J.; Du, X.; Li, J.; Yamagata, N.; Xu, B. Taurine Boosts Cellular Uptake of Small d-Peptides for Enzyme-Instructed Intracellular Molecular Self-Assembly. *J. Am. Chem. Soc.* **2015**, *137*, 10040−10043.
(44) Fujii, N.; Satoh, K.; Harada, K.; Ishibashi, Y. Simultaneous Stereoinversion and Isomerization at Specific Aspartic Acid Residues in αA-Crystallin from Human Lens. *J. Biochem.* **1994**, *116*, 663−669.
(45) Sylvestre, M.; Lv, S.; Yang, L. F.; Luera, N.; Peeler, D. J.; Chen, B.-M.; Roffler, S. R.; Pun, S. H. Replacement of L-amino acid peptides with D-amino acid peptides mitigates anti-PEG antibody generation against polymer-peptide conjugates in mice. *J. Controlled Release* **2021**, *331*, 142−153.
(46) Li, Y.; Han, R.; Chen, M.; Yang, X.; Zhan, Y.; Wang, L.; Luo, X. Electrochemical Biosensor with Enhanced Antifouling Capability Based on Amyloid-like Bovine Serum Albumin and a Conducting Polymer for Ultrasensitive Detection of Proteins in Human Serum. *Anal. Chem.* **2021**, *93*, 14351−14357.

https://doi.org/10.1021/acssensors.2c00518
ACS Sens. 2022, 7, 1740−1746